58906-00-105, 85088-20-105

ANL/CP--75121

DE92 006985

MANUSCRIPT

POSITRON 2D-ACAR EXPERIMENTS AND ELECTRON-POSITRON MOMENTUM DENSITY IN $YBa_2Cu_3O_{7-x}$*

L.C. Smedskjaer,[1] A. Bansil,[3] U. Welp[2], Y. Fang[1], and K.G. Bailey[1]

[1]Materials Science Division, [2]Science & Technology Center for Superconductivity
Argonne National Laboratory, Argonne, IL 60439

[3]Physics Department, Northeastern University, Boston, MA 02115

Proc. Materials Research Society Fall Meeting, December 2-6, 1991, Boston, MA.

jmc

DISCLAIMER

*Work supported by the U.S. Department of Energy, BES-Materials Sciences under contract #W-31-109-ENG-38 (LCS, YF, KGB) and the National Science Foundation Office of Science & Technology Centers under contract #STC-8809854 (UW).

POSITRON 2D-ACAR EXPERIMENTS AND ELECTRON-POSITRON MOMENTUM DENSITY IN $YBa_2Cu_3O_{7-x}$

L.C. Smedskjaer[1], A. Bansil[3], U. Welp[2], Y. Fang[1], and K.G. Bailey[1].

1 Materials Science Division and 2 Science and Technology Center for Superconductivity. Argonne National Laboratory, Argonne, IL 60439.

3 Physics Department, Northeastern University, Boston, Massachusetts 02115

ABSTRACT

We discuss positron annihilation (2D-ACAR) measurements in the c-projection on an *untwinned* metallic single crystal of $YBa_2Cu_3O_{7-x}$ as a function of temperature, for five temperatures ranging from 30K to 300K. The measured 2D-ACAR intensities are interpreted in terms of the electron-positron momentum density obtained within the KKR-band theory framework. The temperature dependence of the 2D-ACAR spectra is used to extract a `background corrected' experimental spectrum which is in remarkable accord with the corresponding band theory predictions, and displays in particular clear signatures of the electron ridge Fermi surface.

Submitted to the MRS meeting in Boston (Fall 1991)

POSITRON 2D-ACAR EXPERIMENTS AND ELECTRON-POSITRON MOMENTUM DENSITY IN $YBa_2Cu_3O_{7-x}$

L.C. Smedskjaer[1], A. Bansil[3], U. Welp[2], Y. Fang[1], and K.G. Bailey[1].
1 Materials Science Division and 2 Science and Technology Center for Superconductivity.
Argonne National Laboratory, Argonne, IL 60439.
3 Physics Department, Northeastern University, Boston, Massachusetts 02115

ABSTRACT

We discuss positron annihilation (2D-ACAR) measurements in the c-projection on an *untwinned* metallic single crystal of $YBa_2Cu_3O_{7-x}$ as a function of temperature, for five temperatures ranging from 30K to 300K. The measured 2D-ACAR intensities are interpreted in terms of the electron-positron momentum density obtained within the KKR-band theory framework. The temperature dependence of the 2D-ACAR spectra is used to extract a `background corrected' experimental spectrum which is in remarkable accord with the corresponding band theory predictions, and displays in particular clear signatures of the electron ridge Fermi surface.

INTRODUCTION

A new chapter in positron studies of superconductors was opened recently when *untwinned* $YBa_2Cu_3O_{7-x}$ specimens were employed. The first announcement of the untwinned 2D-ACAR results was made by the Texas-Livermore effort [1], followed immediately afterwards by the Argonne-Northeastern effort [2]. Most important, the data from these two independent experiments are very similar, and further both groups make a very similar interpretation in terms of the existence of Fermi surfaces in this material. The preliminary results of experiments in Geneva on an untwinned $YBa_2Cu_3O_{7-x}$ single crystal have recently been reported at the Positron Conference in Hungary (ICPA-9) [3], and appear to be consistent with the aforementioned measurements. It is clear that the coming on line of the untwinned specimens marks a significant milestone, and that the application of the 2D-ACAR technique in exploring the Fermiology of the high-T_c's can now go forward with a degree of confidence.

The crucial importance of model theoretical predictions as a basis for interpreting 2D-ACAR spectra has been evident since the inception of this spectroscopy as a tool for investigating the electronic structure and Fermiology of materials.[4,5]. The first theoretical results by Bansil *et al.* [6], using multiple scattering theory (MST) within the KKR scheme, have been followed by a series of theoretical papers by these and other authors[7-11]. The basic band theory predictions for the 2D-ACAR spectrum of $YBa_2Cu_3O_7$, and the Fermi surface (FS) signatures therein, have thus been clarified. This theoretical picture has turned out to be robust in that the results from various groups using different detailed band structure methodologies (LAPW, LMTO, KKR) are quite similar, relatively smaller differences in various first principles computations, arising from those in the underlying band structures, notwithstanding. Consequently, these results may be confronted with experiments with a degree of confidence, and have indeed played an essential role in helping interpret 2D-ACAR spectra in $YBa_2Cu_3O_{7-x}$.

An outline of this article is as follows. The introductory remarks are followed by an overview of the theoretical formulation of the electron-positron momentum density relevant for the discussion of the positron 2D-ACAR spectra. The latest experimental results on untwinned single crystals of $YBa_2Cu_3O_{7-x}$ are then presented and compared with the corresponding band theory predictions, followed by a few concluding remarks.

THEORETICAL OVERVIEW

The spectral quantity of relevance in connection with the 2D-ACAR experiment is the electron-positron momentum density $\rho_{2\gamma}(\mathbf{p})$, which can be expressed in the form

$$\rho_{2\gamma}(\mathbf{p}) = \frac{1}{\pi^2}\int d\mathbf{r}\int d\mathbf{r}' \exp\,[-i\,\mathbf{p}\cdot(\mathbf{r}-\mathbf{r}')]\int dE\, f(E)\int dE_+\, f_+(E_+) \times \mathrm{Im}\, G\,(\mathbf{r},\mathbf{r}';E)\ \mathrm{Im}\, G_+(\mathbf{r},\mathbf{r}';E_+) \qquad (1)$$

in terms of the electron and positron one-particle Green's functions $G(E)$ and $G_+(E)$, and the associated Fermi-Dirac distribution functions $f(E)$ and $f_+(E)$ respectively. Note that Eq. (1) assumes independent particles and implicitly neglects the effects of electron-positron correlations. The 2D-ACAR experiment measures the 2D-projection of $\rho_{2\gamma}(\mathbf{p})$ along a specific direction in momentum space.

Our theoretical treatment is based on the application of multiple-scattering theory techniques to a system of non-overlapping muffin-tin potentials (including 'empty' spheres) to represent the crystal potential. The form of $\rho_{2\gamma}(\mathbf{p})$ for a general lattice with basis may be described most simply in terms of the formula for the electron momentum density $\rho(\mathbf{p})$:[11]

$$\rho(\mathbf{p}) = -\frac{(4\pi)^2}{\tau}\sum_j \frac{f(E)}{(E-p^2)^2}\,\frac{\left|\sum_\mu \exp(-i\mathbf{p}\cdot\mathbf{b}_\mu)\sum_L \bar{C}_{L\mu}(\mathbf{k})\, s_{l\mu}(p,E)\cot\eta_{l\mu}\, Y_L(\mathbf{p})\right|^2}{\sum_{\mu\nu}\sum_{LL'} \bar{C}_{L\mu}(\mathbf{k})\, \dot{M}_{LL'}^{\mu\nu}\, \bar{C}_{L'\nu}(\mathbf{k})} \qquad (2)$$

Here, all vectors and matrices are in the space of angular momentum and basis atom indices L and μ, and are to be evaluated at the energies $E=E_{\mathbf{k},j}$ of the Bloch levels at the reduced wave vector $\mathbf{k}$. $Y_L(\mathbf{p})$ is the Lth real spherical harmonic, τ the unit cell volume, $\mathbf{b}_\mu$ denotes the position, and $\eta_{l\mu}$ the l th phase-shift of the μth atom. $s_{l\mu}(p,E)$ are smoothly varying functions involving the solutions of the radial Schrödinger equation for the μth muffin-tin potential. The remaining quantites are the KKR matrix M and its eigenvectors $C_{L\mu}(\mathbf{k})$. They satisfy the secular equation $MC = 0$. The momentum density of the positron in its ground-state ($\mathbf{k}=0$) is given by a formula similar to Eq. (2), except that in this case there is no summation over j. $\rho_{2\gamma}(\mathbf{p})$ is then obtained straightforwardly as a convolution of the e^- and e^+ momentum density functions, see Mijnarends and Bansil[11] for details.

RESULTS AND DISCUSSION

We discuss 2-D ACAR data in the c-axis projection for *untwinned* $YBa_2Cu_3O_{6.9}$ at temperatures 30 K, 70 K, 100 K, 185 K and 300 K. The total number of counts were 100 Mcounts for the 30K and 300K spectra and 16-22 Mcounts for the remaining spectra. The resolution FWHM due to the camera and the sample size is 0.4-0.5 mrad. At low temperatures this will be the effective resolution, while the thermal velocity of the positron gives rise to resolution broadening at higher temperatures. Assuming an effective positron mass of one, the effective resolution at 300K is 0.7 mrad. All observed spectra were shown to possess C_{2v} symmetry, and were subsequently symmetrized accordingly in order to augment statistical precision [12].

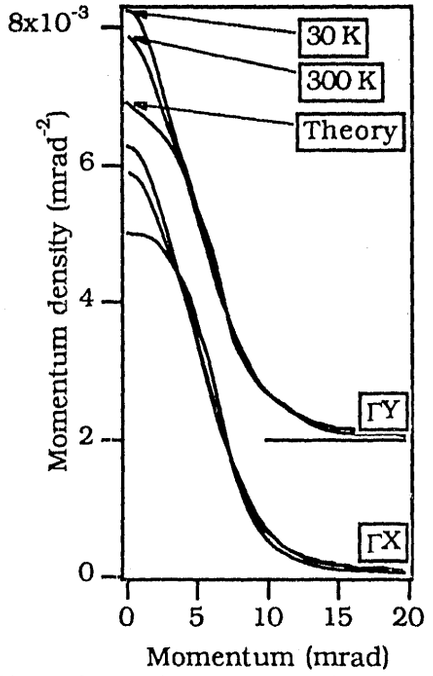

Fig. 1. Comparison of two sections through the data with corresponding theoretical results of Bansil *et al.* [7].

The sample was an *untwinned* single crystal of $YBa_2Cu_3O_{6.9}$ (0.9 x 1.6 x 0.1 mm^3) with a transition temperature of 91K and a transition width of 1K. The sample was supported by a 25 μm dia. tungsten wire. Based upon separate experiments we estimate the background contribution from the sample support to be 5-10% of the annihilations. The crystal c-axis was oriented *in situ*, while the precise a (b) axis orientation was deduced from the data

The data possess a temperature dependence as illustrated by Fig. 1 which shows sections along ΓX and ΓY in the measured 2D-ACAR spectrum. The temperature dependence is "negative" in the sense that the top counts in the curve decreases with increasing temperature. In Fig. 1 only the extreme temperatures are shown, the remaining observations fall in between these extremes. Similar temperature effects have also been reported for *twinned*

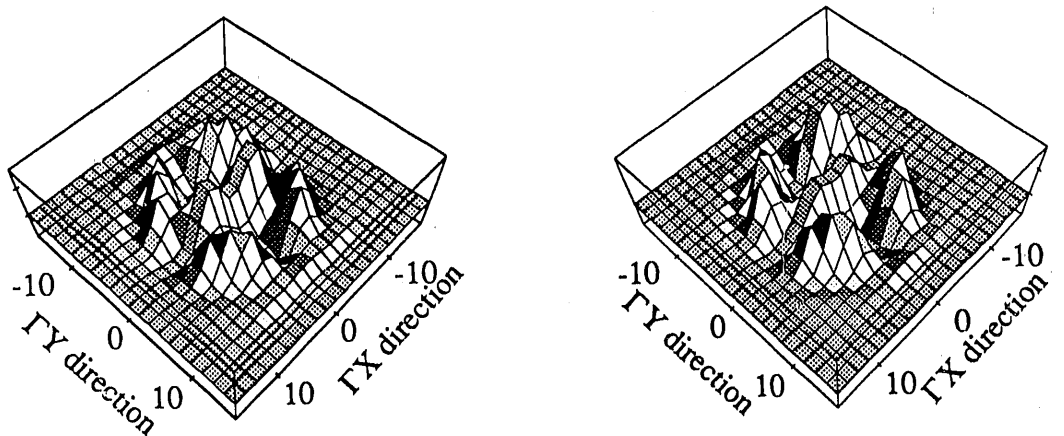

Fig. 2. Anisotropic part of 2D-ACAR data for the untwinned sample. Left: 300K, right: 30K. The pixel size is 1.57 by 1.57 mrad, which is about twice the resolution (FWHM) at 300K.

samples [13] as well as for polycrystalline samples for temperatures above T_c [14, 15]. In comparing measurements with the corresponding band theory predictions [7], Fig. 1 shows that the theory and experiment differ for low momenta; this type of discrepancy also exists in earlier data from *twinned* specimens (e.g., [7,16]), where it was suggested to be the result of a `background' spectrum caused possibly by annihilations in positron traps and/or sample support. We return below to the question of obtaining a suitable `background corrected' experimental spectrum in terms of the present temperature dependent 2D-ACAR spectra.

In Fig. 2 the anisotropic parts of the spectra, obtained by subtracting smooth isotropic functions from the observed data, are shown for the untwinned sample; the smooth functions used here were constrained to be less than the measured spectrum at all momenta. (Spectra obtained at intermediate temperatures fall in between the results of Fig. 2, and are not shown.) It is seen that the anisotropic part consists of two main features, namely a central ridge in the ΓX direction, and four mountains surrounding the ridge. In addition, a sideridge, running parallel to the ΓX direction at 13 mrad, is seen as well. In a *twinned* crystal the four mountains are present [2] ,but the central ridge takes the form of a blurred cross. It can be shown that the ridge and the sideridges possess C_{2v} symmetry while the mountains are almost C_{4v} symmetric. Physically, the ridge and sideridge features arise mainly from electronic states associated with the CuO chains, while the mountains can be due to both the chain states and the CuO plane states.Although the major features are similar, changes in the details of the spectral shapes are nevertheless apparent with temperature most notably the changes in the shape of the central ridge in Fig. 2.

In order to understand the temperature dependent data, we investigated the possible existence of linear dependencies in the spectra. We found that the spectra possess linear dependencies in the sense that any spectrum, $M(\mathbf{p},T)$, could to a good approximation be written as

$$M(\mathbf{p},T) \approx (1-I(T))\, F(\mathbf{p}) + I(T)\, B(\mathbf{p}) \qquad (3)$$

where $F(\mathbf{p})$ and $B(\mathbf{p})$ are two *temperature independent* spectra, while I(T) is a *temperature dependent* weight factor. The form (3) shows that the observed spectra are a linear combination of two different types of annihilation spectra, one ($F(\mathbf{p})$) being due to annihilations in the 'ideal' material, the other ($B(\mathbf{p})$) possibly due to annihilations in less perfect sample regions.

The question now arises whether the spectrum $F(\mathbf{p})$ is similar to that predicted by band theory. If this is the case, then it should be possible to write the theoretical spectrum $T(\mathbf{p})$ on the form

$$T(\mathbf{p}) \approx (1-\gamma)\, M(\mathbf{p},T_1) + \gamma\, M(\mathbf{p},T_2) \qquad (4)$$

where γ is a parameter to be determined by a least squares fit. It is noted, that if the hypothesis that $F(\mathbf{p}) \approx T(\mathbf{p})$ is wrong, then a good fit cannot be obtained. In order to obtain good statistics we choose the 30K and 300K spectra for the fitting procedure and obtained the 'background corrected' spectrum $H(\mathbf{p})$ as:

$$H(\mathbf{p}) = (1-\tilde{\gamma})\, M(\mathbf{p},T_1) + \tilde{\gamma}\, M(\mathbf{p},T_2) \qquad (5)$$

where $\tilde{\gamma}$ is the value obtained from the least squares fit. In Fig. 3 the resulting H(**p**) is compared to T(**p**) for many directions in momentum space.

A comparison between Fig. 3 and Fig. 1 shows a dramatic improvement with regard to the agreement between theory and experiment. It is noteworthy that the as observed data in Fig. 1 displays rather similar behaviors along the ΓX and ΓY directions; the background corrected data on the other hand exhibit a strong anisotropy near the center in good agreement with the band theory predictions. The origin of the background term is not clear, although shallow trapping is a possibility. We now turn to studying the Fermiology related features in H(**p**) and compare them to the band theoretical predictions. Here we will consider the anisotropic difference curves obtained by subtracting data from two different directions from one another.

Figure 4(a) displays typical theoretical difference sections. The complicated structure of the curves reflects the character of both the partially filled bands which give Fermi surface breaks, as well as the completely filled bands which yield more smooth variations in the momentum density. Recall that the Fermi surface of $YBa_2Cu_3O_7$ is predicted by band theory to consist of four sheets, the 'electron ridge', the 'pillbox', and two closely placed 'barrels'. The signatures of the electron ridge Fermi surface are the break around r_0 in the first Brillouin zone (the break at the reflected point $-r_0$ not shown), its first 'umklapp' image (r_1,r_2) around 6.3 mrad, and the second image (r_3,r_4) around 12.6 mrad. [For orientation, the Brillouin zone dimension is 6.3 mrad in $YBa_2Cu_3O_7$.] The ridge Fermi surface arises from a highly anisotropic one-dimensional band which is essentially full along ΓX but nearly empty along the ΓY direction. The associated electronic states couple strongly with the positron state in $YBa_2Cu_3O_7$ and yield clear features of the sort

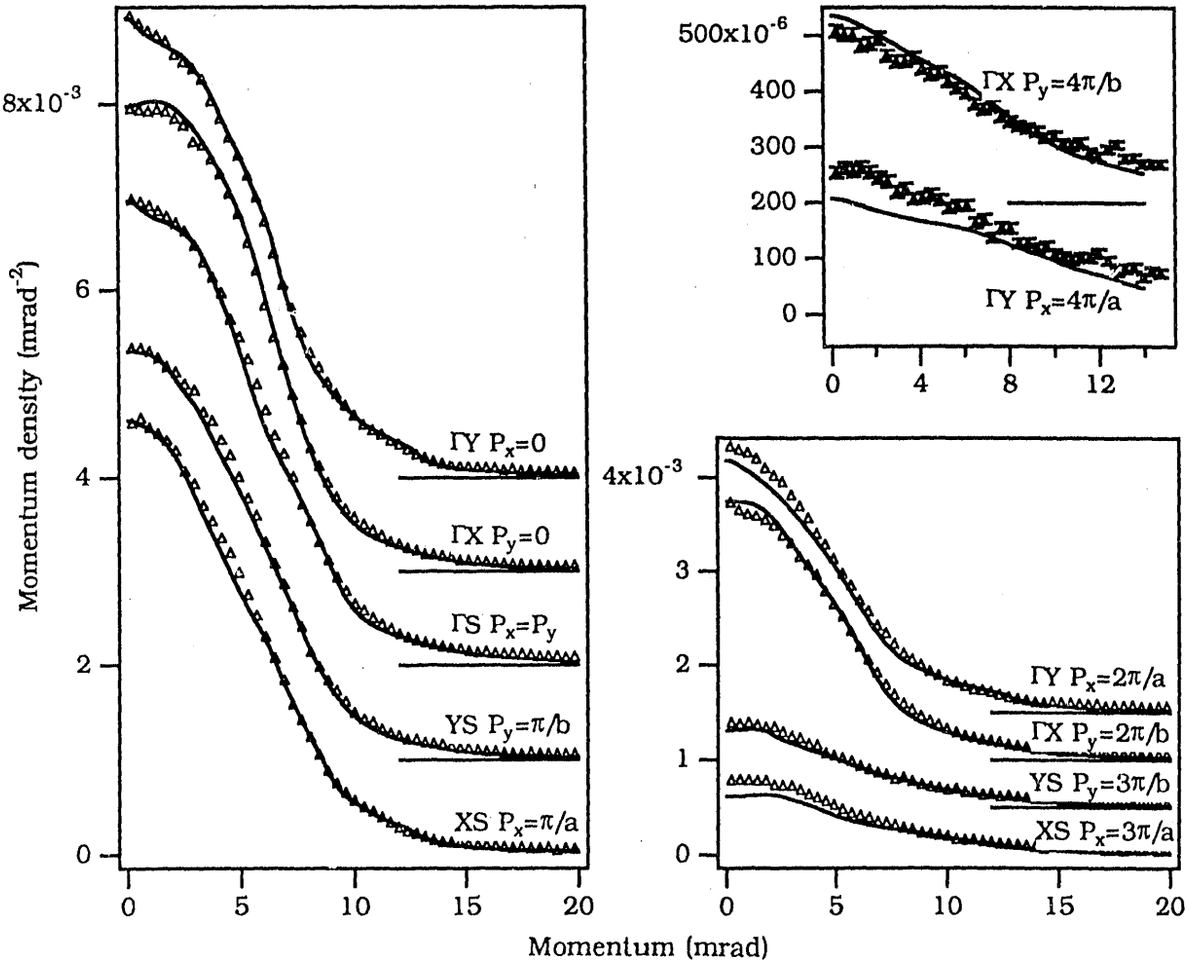

Fig. 3 A comparison of various sections through the background corrected 2D-ACAR spectrum, H(**p**), for an *untwinned* $YBa_2Cu_3O_{7-x}$ sample with the corresponding theoretical predictions of Bansil *et al.* [7].

seen in Fig. 4(a). We also see other Fermi surface features in Fig. 4(a); most notably the breaks denoted by (s_1, s_2, s_3, s_4) and the related images (s_5,s_6) in the lowest panel, all arising from a small hole Fermi surface (the pillbox sheet) centered around the symmetry point S. The larger hole sheets, also centered around S, arising from the Cu-O planes (the barrel sheets) do not couple well with the positron wave function in $YBa_2Cu_3O_7$ and are not expected to give substantial signals in the 2D-momentum density.

Fig. 4(b) shows that experimental anisotropies are in good accord with theory with regard to both the details of the spectral features, and also the absolute magnitude of the overall undulations. The level of discrepancies seen here is common in even simpler materials in first principles comparisons between theory and experiment. If the experimental 2D-ACAR is not corrected for background, the shapes of the anisotropic spectra are quite similar to those shown in Fig. 4(b), but the absolute size of the measured anisotropy is only about half as large as theory. Notably, in a twinned crystal, the XS-YS and ΓY-ΓX anisotropy is zero, and ΓS-ΓX is identical to ΓS-ΓY. Therefore important aspects of the momentum density simply cannot be probed via measurements on twinned crystals.

FS signatures in the experimental spectra can now be elucidated with reference to Fig. 4. We consider the ridge FS first. As noted above, the ridge FS gives three distinct features: (i) rapid variation in anisotropy near p=0, (ii) an image around 6.3 mrad, and (iii) a second image around 13 mrad. The experimental spectra display all three of these features. Near p=0 both sets of curves in Fig. 4(b) possess similarly rapid variations and slopes; the width of the experimental ridge would however appear to be somewhat larger than that implicit in our band structure. The 6.3 mrad image of the ridge (r_1,r_2) is particularly important in the ΓY-ΓX curve because this feature lies on a relatively gently varying background and remains quite prominent in the theory even after including resolution broadening, and it is crucial that this feature is indeed observed clearly in the

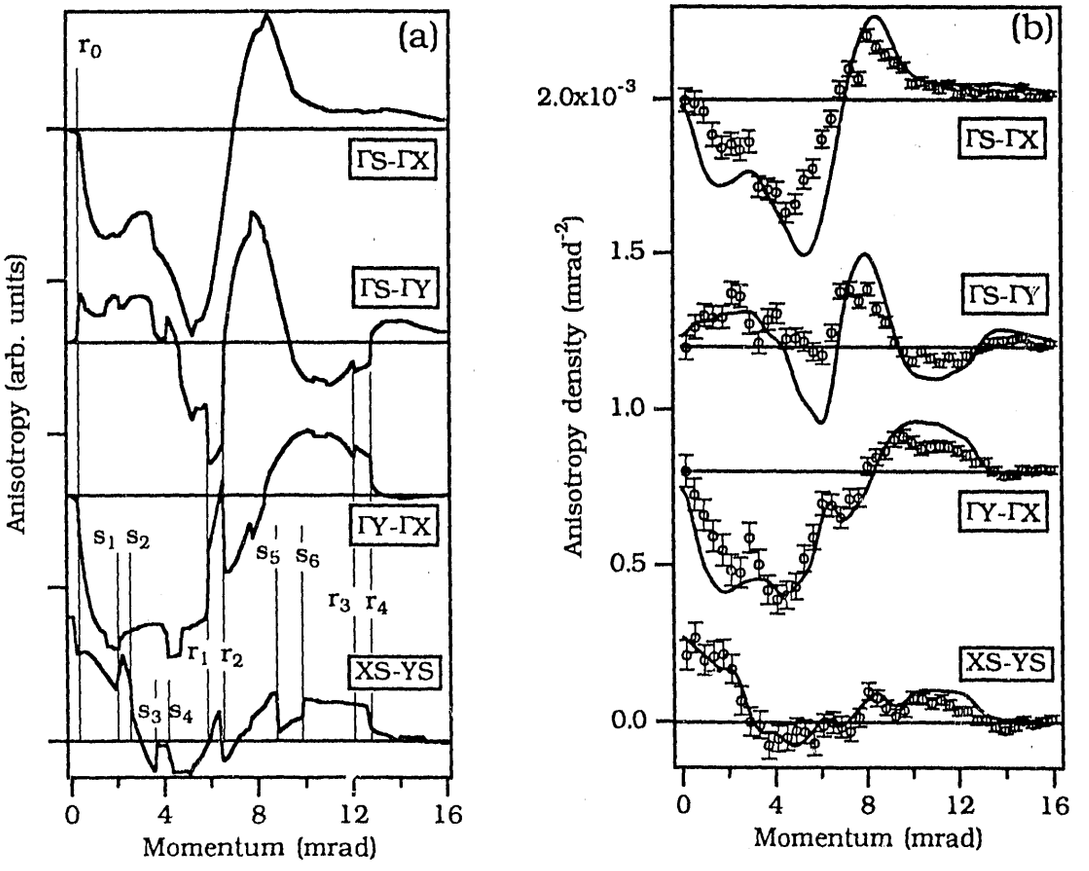

Fig. 4 (a): Theoretical anisotropic momentum distribution, here defined by taking differences between spectra along four different pairs of directions. Thin vertical lines mark the position of various FS features r_0, s_1, etc. discussed in the text. (b) A comparison between the resolution broadened theory curves in (a) with the corresponding experimental difference sections obtained from the corrected data H(**p**).

experimental data. By contrast, in the ΓS-ΓY curve, the resolution broadening effects would make the 6.3 mrad ridge image difficult to distinguish from the background. Finally, the image of the ridge FS near 13 mrad (r_3,r_4) becomes rather smooth in theory upon resolution broadening. We emphasize however that the experimental data in this momentum range is quite consistent with the theory. (In particular, if theory and experiment are renormalized to agree in the region from 8 to 16 mrad, then the experimental edge around 13 mrad is just about as sharp as that predicted theoretically.) Also, in the case of ΓS-ΓY, both theory and experiment show the related zero crossing around 13 mrad. Concerning the 'pillbox', the prominent features involve the XS-YS anisotropic spectrum, where the theory and experiment appear to be in accord in Fig. 4(b), although upon resolution broadening, the theoretical breaks s_1 through s_4 become rather indistinct, and are difficult to identify in the experimental spectra. The dip arising from the breaks s_5 and s_6 remains distinct even after resolution effects are included, and in this momentum region, the experimental data indeed clearly display a similar dip in accord with the theory. Further analysis of the 2D-ACAR data is nevertheless needed to firmly establish the existence of the pillbox FS via the present experiments.

CONCLUSIONS:

In summary, we have discussed temperature dependent 2D-ACAR positron experiments on an untwinned single crystal of metallic $YBa_2Cu_3O_{7-x}$. After a suitable background correction, the experimental spectra are in remarkable agreement with the corresponding band theory predictions. The absolute amplitudes and spectral shapes of the anisotropies observed experimentally for a number of typical sections are reproduced quite well by the band theory. Several theoretically predicted characteristic signatures of the ridge Fermi surface are clearly present in the data; further analysis of the data may help identify other FS signatures in the spectra. The present information concerning the Fermi surface from the positron spectroscopy, when combined with complementary results from angle-resolved photoemission (which firmly show the Cu-O plane sheets)[17], and the dHvA experiments (which indicate the pillbox FS)[18], offer rather strong evidence that the Fermi surface of normal state $YBa_2Cu_3O_7$ is in essential accord with the band theory predictions.

ACKNOWLEDGMENTS:

The present work was supported by the U.S. Department of Energy, Basic Energy Sciences, Division of Materials Sciences under contract #W-31-109- ENG-38 (LS, YF, KB), including a subcontract to Northeastern University (AB), and the National Science Foundation's Office of Science and Technology Centers under contract #STC-8809854 (UW). This work benefited from the allocation of supercomputer time on the NERSC and San Diego Supercomputer centers.

REFERENCES

[1] H. Haghighi *et al.* , Phys. Rev. Letters 67, 382 (1991)., and J. Phys. and Chem. of Solids (1991)
[2] L.C Smedskjaer., *et al.*, J. Phys. and Chem. of Solids, (1991).
[3] L. Hoffmann, W. Sadowski, and M. Peter, Proc. of the 9'th "Int. Conf. on Positron Annihilation", Hungary (1991); to appear as a special vol. of Mat. Sci. Forum (1992)
[4] S. Berko in, Momentum Distributions, edited by R. N. Silver and P. E. Sokol, (Plenum, New York, 1989), pp. 273.
[5] P. E. Mijnarends, in Positron Solid State Physics, Course LXXXIII, Int. School of Phys. "Enrico Fermi", edited by : W.Brandt and A. Dupasquier, (North-Holland ,1983), pp. 146
[6] A. Bansil *et al.* Phys. Rev. Lett. 61, 2480 (1988).
[7] A. Bansil, P. E. Mijnarends, and L. C. Smedskjaer, Physica C 172, 175 (1990).
[8] A. Bansil, P. E. Mijnarends, and L. C. Smedskjaer, Phys. Rev. B 43, 3667 (1991).
[9] S. Massidda, Physica C 169, 137 (1990); T. Jarlborg *et al.* , J. Phys. Chem. Solids (1991).
[10] D. Singh *et al.* , Phys. Rev. B 42, 2696 (1990).
[11] P.E. Mijnarends and A. Bansil, J. Phys.: Conden. Matter 2, 911 (1990)
[12] L.C.Smedskjaer, and D.G.Legnini , Nucl. Inst. Meth. Phys. Res., A 292, 487,(1990)
[13] L. Hoffmann *et al.* J. Phys. and Chem. of Solids, (1991)
[14] L.C. Smedskjaer *et al.* Physica B 150, 56 (1988)
[15] E.C. von Stetten *et al.* Phys. Rev. Lett. 60, 2198 (1988).
[16] B. Barbiellini, *et al.* Phys Rev B 43, 7810 (1991).
[17] J.C. Campuzano *et al.* Phys. Rev. B 43, 2788 (1991)
[18] F.M. Mueller J. Phys. Chem. Solids (1991); G. Kido *et al.* J. Phys. Chem. Solids (1991)

END

DATE
FILMED
2/27/92